EUROPEAN ORGANISATION FOR NUCLEAR RESEARCH

A Study of QCD Structure Constants and a Measurement of $\alpha_s(M_{\mathrm{Z}^0})$ at LEP using Event Shape Observables

The OPAL Collaboration

Abstract

The dependence of event shape cross sections on the QCD structure constants C_A, C_F and T_F is studied using data from the OPAL detector at LEP. The observables Thrust, Heavy Jet Mass, Total and Wide Jet Broadening are used. They allow the use of $\mathcal{O}(\alpha_s^2)$, resummed NLLA, and combined $\mathcal{O}(\alpha_s^2)$ plus resummed NLLA QCD calculations so that a comparison between the different approaches can be performed. The measured values of the structure constants are found to be consistent with standard QCD based on SU(3) and five active quark flavours. A measurement of the strong coupling constant using NLLA QCD calculations alone results in $\alpha_s(M_{\mathrm{Z}^0}) = 0.113^{+0.009}_{-0.008}$, which complements our previous determinations.

The OPAL Collaboration

R. Akers[16], G. Alexander[23], J. Allison[16], N. Altekamp[5], K. Ametewee[25], K.J. Anderson[9],
S. Anderson[12], S. Arcelli[2], S. Asai[24], D. Axen[29], G. Azuelos[18,a], A.H. Ball[17], E. Barberio[26],
R.J. Barlow[16], R. Bartoldus[3], J.R. Batley[5], G. Beaudoin[18], S. Bethke[14], A. Beck[23],
G.A. Beck[13], C. Beeston[16], T. Behnke[27], K.W. Bell[20], G. Bella[23], S. Bentvelsen[8],
P. Berlich[10], J. Bechtluft[14], O. Biebel[14], I.J. Bloodworth[1], P. Bock[11], H.M. Bosch[11],
M. Boutemeur[18], S. Braibant[12], P. Bright-Thomas[25], R.M. Brown[20], A. Buijs[8],
H.J. Burckhart[8], R. Bürgin[10], C. Burgard[27], P. Capiluppi[2], R.K. Carnegie[6], A.A. Carter[13],
J.R. Carter[5], C.Y. Chang[17], C. Charlesworth[6], D.G. Charlton[1,b], S.L. Chu[4],
P.E.L. Clarke[15], J.C. Clayton[1], S.G. Clowes[16], I. Cohen[23], J.E. Conboy[15], O.C. Cooke[16],
M. Cuffiani[2], S. Dado[22], C. Dallapiccola[17], G.M. Dallavalle[2], C. Darling[31], S. De Jong[12],
L.A. del Pozo[8], H. Deng[17], M.S. Dixit[7], E. do Couto e Silva[12], J.E. Duboscq[8],
E. Duchovni[26], G. Duckeck[8], I.P. Duerdoth[16], U.C. Dunwoody[8], J.E.G. Edwards[16],
P.G. Estabrooks[6], H.G. Evans[9], F. Fabbri[2], B. Fabbro[21], M. Fanti[2], P. Fath[11], F. Fiedler[12],
M. Fierro[2], M. Fincke-Keeler[28], H.M. Fischer[3], R. Folman[26], D.G. Fong[17], M. Foucher[17],
H. Fukui[24], A. Fürtjes[8], P. Gagnon[6], A. Gaidot[21], J.W. Gary[4], J. Gascon[18], N.I. Geddes[20],
C. Geich-Gimbel[3], S.W. Gensler[9], F.X. Gentit[21], T. Geralis[20], G. Giacomelli[2],
P. Giacomelli[4], R. Giacomelli[2], V. Gibson[5], W.R. Gibson[13], J.D. Gillies[20], J. Goldberg[22],
D.M. Gingrich[30,a], M.J. Goodrick[5], W. Gorn[4], C. Grandi[2], E. Gross[26], G.G. Hanson[12],
M. Hansroul[8], M. Hapke[13], C.K. Hargrove[7], P.A. Hart[9], C. Hartmann[3], M. Hauschild[8],
C.M. Hawkes[8], R. Hawkings[8], R.J. Hemingway[6], G. Herten[10], R.D. Heuer[8], J.C. Hill[5],
S.J. Hillier[8], T. Hilse[10], P.R. Hobson[25], D. Hochman[26], R.J. Homer[1], A.K. Honma[28,a],
R. Howard[29], R.E. Hughes-Jones[16], D.E. Hutchcroft[5], P. Igo-Kemenes[11], D.C. Imrie[25],
A. Jawahery[17], P.W. Jeffreys[20], H. Jeremie[18], M. Jimack[1], A. Joly[18], M. Jones[6],
R.W.L. Jones[8], P. Jovanovic[1], D. Karlen[6], J. Kanzaki[24], K. Kawagoe[24], T. Kawamoto[24],
R.K. Keeler[28], R.G. Kellogg[17], B.W. Kennedy[20], B.J. King[8], J. King[13], J. Kirk[29],
S. Kluth[5], T. Kobayashi[24], M. Kobel[10], D.S. Koetke[6], T.P. Kokott[3], S. Komamiya[24],
R. Kowalewski[8], T. Kress[11], P. Krieger[6], J. von Krogh[11], P. Kyberd[13], G.D. Lafferty[16],
H. Lafoux[8], R. Lahmann[17], W.P. Lai[19], D. Lanske[14], J. Lauber[8], J.G. Layter[4], A.M. Lee[31],
E. Lefebvre[18], D. Lellouch[26], J. Letts[2], L. Levinson[26], S.L. Lloyd[13], F.K. Loebinger[16],
G.D. Long[17], B. Lorazo[18], M.J. Losty[7], J. Ludwig[10], A. Luig[10], A. Malik[21], M. Mannelli[8],
S. Marcellini[2], C. Markus[3], A.J. Martin[13], J.P. Martin[18], T. Mashimo[24], W. Matthews[25],
P. Mättig[3], J. McKenna[29], E.A. Mckigney[15], T.J. McMahon[1], A.I. McNab[13], F. Meijers[8],
S. Menke[3], F.S. Merritt[9], H. Mes[7], A. Michelini[8], G. Mikenberg[26], D.J. Miller[15], R. Mir[26],
W. Mohr[10], A. Montanari[2], T. Mori[24], M. Morii[24], U. Müller[3], B. Nellen[3], B. Nijjhar[16],
S.W. O'Neale[1], F.G. Oakham[7], F. Odorici[2], H.O. Ogren[12], N.J. Oldershaw[16],
C.J. Oram[28,a], M.J. Oreglia[9], S. Orito[24], F. Palmonari[2], J.P. Pansart[21], G.N. Patrick[20],
M.J. Pearce[1], P.D. Phillips[16], J.E. Pilcher[9], J. Pinfold[30], D.E. Plane[8], P. Poffenberger[28],
B. Poli[2], A. Posthaus[3], T.W. Pritchard[13], H. Przysieznizak[30], M.W. Redmond[8], D.L. Rees[1],
D. Rigby[1], M.G. Rison[5], S.A. Robins[13], N. Rodning[30], J.M. Roney[28], E. Ros[8], A.M. Rossi[2],
M. Rosvick[28], P. Routenburg[30], Y. Rozen[8], K. Runge[10], O. Runolfsson[8], D.R. Rust[12],

M. Sasaki[24], C. Sbarra[2], A.D. Schaile[8], O. Schaile[10], F. Scharf[3], P. Scharff-Hansen[8], P. Schenk[4], B. Schmitt[3], M. Schröder[8], H.C. Schultz-Coulon[10], P. Schütz[3], M. Schulz[8], J. Schwiening[3], W.G. Scott[20], M. Settles[12], T.G. Shears[16], B.C. Shen[4], C.H. Shepherd-Themistocleous[7], P. Sherwood[15], G.P. Siroli[2], A. Skillman[15], A. Skuja[17], A.M. Smith[8], T.J. Smith[28], G.A. Snow[17], R. Sobie[28], S. Söldner-Rembold[10], R.W. Springer[30], M. Sproston[20], A. Stahl[3], M. Starks[12], C. Stegmann[10], K. Stephens[16], J. Steuerer[28], B. Stockhausen[3], D. Strom[19], P. Szymanski[20], R. Tafirout[18], P. Taras[18], S. Tarem[26], M. Tecchio[9], P. Teixeira-Dias[11], N. Tesch[3], M.A. Thomson[8], E. von Törne[3], S. Towers[6], M. Tscheulin[10], T. Tsukamoto[24], A.S. Turcot[9], M.F. Turner-Watson[8], P. Utzat[11], R. Van Kooten[12], G. Vasseur[21], P. Vikas[18], M. Vincter[28], F. Wäckerle[10], A. Wagner[27], D.L. Wagner[9], C.P. Ward[5], D.R. Ward[5], J.J. Ward[15], P.M. Watkins[1], A.T. Watson[1], N.K. Watson[7], P. Weber[6], P.S. Wells[8], N. Wermes[3], B. Wilkens[10], G.W. Wilson[27], J.A. Wilson[1], T. Wlodek[26], G. Wolf[26], S. Wotton[11], T.R. Wyatt[16], G. Yekutieli[26], V. Zacek[18], W. Zeuner[8], G.T. Zorn[17].

[1]School of Physics and Space Research, University of Birmingham, Birmingham B15 2TT, UK
[2]Dipartimento di Fisica dell' Università di Bologna and INFN, I-40126 Bologna, Italy
[3]Physikalisches Institut, Universität Bonn, D-53115 Bonn, Germany
[4]Department of Physics, University of California, Riverside CA 92521, USA
[5]Cavendish Laboratory, Cambridge CB3 0HE, UK
[6]Carleton University, Department of Physics, Colonel By Drive, Ottawa, Ontario K1S 5B6, Canada
[7]Centre for Research in Particle Physics, Carleton University, Ottawa, Ontario K1S 5B6, Canada
[8]CERN, European Organisation for Particle Physics, CH-1211 Geneva 23, Switzerland
[9]Enrico Fermi Institute and Department of Physics, University of Chicago, Chicago IL 60637, USA
[10]Fakultät für Physik, Albert Ludwigs Universität, D-79104 Freiburg, Germany
[11]Physikalisches Institut, Universität Heidelberg, D-69120 Heidelberg, Germany
[12]Indiana University, Department of Physics, Swain Hall West 117, Bloomington IN 47405, USA
[13]Queen Mary and Westfield College, University of London, London E1 4NS, UK
[14]Technische Hochschule Aachen, III Physikalisches Institut, Sommerfeldstrasse 26-28, D-52056 Aachen, Germany
[15]University College London, London WC1E 6BT, UK
[16]Department of Physics, Schuster Laboratory, The University, Manchester M13 9PL, UK
[17]Department of Physics, University of Maryland, College Park, MD 20742, USA
[18]Laboratoire de Physique Nucléaire, Université de Montréal, Montréal, Quebec H3C 3J7, Canada
[19]University of Oregon, Department of Physics, Eugene OR 97403, USA
[20]Rutherford Appleton Laboratory, Chilton, Didcot, Oxfordshire OX11 0QX, UK

[21]CEA, DAPNIA/SPP, CE-Saclay, F-91191 Gif-sur-Yvette, France
[22]Department of Physics, Technion-Israel Institute of Technology, Haifa 32000, Israel
[23]Department of Physics and Astronomy, Tel Aviv University, Tel Aviv 69978, Israel
[24]International Centre for Elementary Particle Physics and Department of Physics, University of Tokyo, Tokyo 113, and Kobe University, Kobe 657, Japan
[25]Brunel University, Uxbridge, Middlesex UB8 3PH, UK
[26]Particle Physics Department, Weizmann Institute of Science, Rehovot 76100, Israel
[27]Universität Hamburg/DESY, II Institut für Experimental Physik, Notkestrasse 85, D-22607 Hamburg, Germany
[28]University of Victoria, Department of Physics, P O Box 3055, Victoria BC V8W 3P6, Canada
[29]University of British Columbia, Department of Physics, Vancouver BC V6T 1Z1, Canada
[30]University of Alberta, Department of Physics, Edmonton AB T6G 2J1, Canada
[31]Duke University, Dept of Physics, Durham, NC 27708-0305, USA

[a]Also at TRIUMF, Vancouver, Canada V6T 2A3
[b] Royal Society University Research Fellow

1   Introduction

The theory of the strong interaction, Quantum Chromo Dynamics (QCD), includes four fundamental vertices involving quarks and gluons. Three of these contribute to the process $e^+e^- \rightarrow$ hadrons in $\mathcal{O}(\alpha_s)$ or in $\mathcal{O}(\alpha_s^2)$ and will be studied here. The fourth is the four gluon vertex, which is an $\mathcal{O}(\alpha_s^2)$ process by itself and contributes only in $\mathcal{O}(\alpha_s^3)$ to e^+e^- annihilation. The three relevant fundamental processes are the splitting of a quark into a quark and a gluon (gluon bremsstrahlung), the splitting of a gluon into a pair of gluons (triple gluon vertex TGV) and the splitting of a gluon into a quark-antiquark pair. The relative strengths of the three processes are determined by the group structure of the theory and are expressed in terms of the numerical values of the QCD structure constants C_F, C_A and T_F, respectively [1]. The splitting of gluons into quark-antiquark pairs contributes with strength T_F for each active quark flavour (counted by N_f), i.e. this process effectively contributes with strength $T_R \equiv T_F N_f$. The choice of SU(3) as the particular group symmetry for QCD requires C_F, C_A and T_F to be $\frac{4}{3}$, 3 and $\frac{1}{2}$, respectively.

The first tests of the gauge structure of QCD at LEP were based on a comparison of angular correlations in 4-jet events with predictions from Monte Carlo simulations [2,3]. In these studies, the data were found to be consistent with QCD, but disfavoured an Abelian gluon model $U(1)_3$ in which the triple gluon vertex is absent. In further studies at LEP [4–7], $\mathcal{O}(\alpha_s^2)$ QCD predictions for the 4-jet cross section were decomposed into structure factor ratios proportional to C_A/C_F and T_F/C_F, assuming $N_f = 5$. They were then fitted to data using observables constructed from angular correlations between the jets. The results yielded values for C_A/C_F and T_F/C_F which were consistent with the QCD ones, while they excluded all other candidate gauge theories with three colour degrees-of-freedom with a high level of significance. However, as QCD matrix elements have been fully computed only up to $\mathcal{O}(\alpha_s^2)$ and a 4-jet event involves at least two QCD vertices, no higher order corrections to the 4-jet cross sections were accounted for in such analyses.

It has been pointed out in [8] that the leading order predictions for 4-jet processes and the next to leading order corrections to 3-jet processes behave in a similar manner with respect to the structure constants. To $\mathcal{O}(\alpha_s)$, the 3-jet cross section consists of the QCD process of gluon bremsstrahlung. Corrections to $\mathcal{O}(\alpha_s^2)$ are given by all three QCD processes at the tree level, and by virtual gluon and quark loops and virtual gluon exchanges in the 3-jet final state. It turns out that the $\mathcal{O}(\alpha_s^2)$ corrections to the 3-jet cross section, including the virtual corrections, can be decomposed into three terms proportional to the three structure constants C_F, C_A and T_F and an overall factor C_F. This means that it should, in principle, be possible to extract measurements of the structure constants from fits to observables dominated by three-jet production. A first attempt to extract the QCD structure constants from event shape observables is described in [8]. This attempt was based on $\mathcal{O}(\alpha_s^2)$ fits to the OPAL data published in [9].

As in the case of the 4-jet based measurements, no higher order corrections to the relative contributions of the fundamental processes are present in the $\mathcal{O}(\alpha_s^2)$ calculations. However, some event shape cross sections have been calculated in the Next-to-Leading-Log

Approximation (NLLA), where emission of soft gluons from the original quark antiquark pair is considered up to all orders by resumming large logarithms. These predictions also depend explicitly on the three structure constants, and therefore permit investigation of the influence of higher orders in the determination of structure constants.

In this study we use event shape observables for which both $\mathcal{O}(\alpha_s^2)$ and NLLA calculations exist. The analysis is performed using data collected with the OPAL detector at LEP. The observables for which the NLLA calculations are most complete are Thrust, Heavy Jet Mass and the Total and Wide Jet Broadening. Beyond the use of the $\mathcal{O}(\alpha_s^2)$ and NLLA calculations separately, the two can be matched to give a third theoretical description of the event shape cross sections which is valid over a wider range. First, we investigate measurements of $\alpha_s(M_{Z^0})$ using the NLLA calculations and compare with our previous $\mathcal{O}(\alpha_s^2)$ and $\mathcal{O}(\alpha_s^2)$+NLLA results from [10]. We then examine all three types of calculations for the QCD structure constant fits.

This paper is mostly a continuation of the studies started in [10] and some symbols and terms used here are defined in [10]. In section 2 experimental details of this study are presented, followed in section 3 by a description of the QCD calculations used for our measurements. In section 4 our measurement of the value of the strong coupling $\alpha_s(M_{Z^0})$ is given. The study of QCD structure constants is presented in section 5. Our conclusions are given in section 6.

2   Experimental Procedure

We consider the four event shape observables Thrust T [11], Heavy Jet Mass based on the Thrust axis M_H [11], Total and Wide Jet Broadening B_T and B_W [12]. A detailed definition of the observables can be found in [10]. The generic observable y is used to denote the observables $1 - T$, $M_H/\sqrt{s}$, B_T and B_W. They are defined such that $y \to 0$ for 2-jet configurations.

A detailed description of the OPAL detector can be found in reference [13]. Here we will briefly describe the parts of the detector relevant to this analysis. Charged tracks are measured using drift chamber systems consisting of a precision vertex chamber, a large jet chamber and Z-chambers outside the jet chamber. The drift chambers are situated in a magnetic field of 0.435 T. Outside the solenoidal magnet coil is the electromagnetic calorimeter, which covers 98% of 4π with 11 704 lead glass blocks. In addition to measuring electrons and photons, it records a significant fraction of the energy of charged and neutral hadrons.

We use the same data as in [10] corrected for effects of the detector, acceptance of selection cuts and initial state radiation. The data sample consists of 336 247 multihadronic events recorded by OPAL in 1990-1991. This data sample is sufficient since statistical uncertainties do not dominate the errors in our study.

In order to compare our data with the perturbative QCD calculations, it is necessary to apply corrections, using Monte Carlo simulations, for the non-perturbative transition of partons to hadrons. We define an event at the *parton level* to consist of the quarks and

gluons that remain after the perturbative evolution has terminated. At the *hadron level* an event consists of the stable hadrons formed in the hadronisation process or through resonance decay.

The NLLA calculations are most applicable for small values of the observables y, but this is also where the effects of hadronisation are larger and less certain. The correction procedure adopted here is as follows. The correction for the effects of hadronisation is performed by convolving the parton-level prediction of QCD with a matrix derived from comparing hadron- and parton-level distributions of the observables from Monte Carlo simulations. This *hadronisation matrix* consists of the probabilities P_{ij} that an event in some bin i at the parton level lies in bin j at the hadron level. With the procedure we adopt here, we compute new correction matrices for several variants of the hadronisation model as a means of assessing systematic uncertainties.

The theoretical predictions convolved with the hadronisation matrix are fitted to the data by a least-χ^2 method where the full covariance matrices are available for the data distributions. The value of $\alpha_s(M_{Z^0})$ and one of the three structure constants are varied in the fits. In the case of the $\mathcal{O}(\alpha_s^2)$ fits, the renormalisation scale factor x_μ (as defined in section 3.1) for each observable is allowed to vary as well. The relative contribution of gluon splitting into quark-antiquark pairs is fitted in terms of N_f assuming $T_F = \frac{1}{2}$, but the results can always be converted into values for T_F assuming $N_f = 5$, using $T_R = N_f T_F$. The ranges of the observables over which the fits are carried out are determined in a way similar to reference [10]. We require that the hadronisation corrections be reasonably small and uniform over the fit range and that the χ^2/d.o.f. values of the fits not vary abruptly when a bin is included or removed from the fit range. The fit ranges are summarised in table 1.

It is convenient to discuss the treatment of systematic uncertainties at this point, because we will follow the same procedures in the two analyses presented in this paper. The systematic uncertainties are estimated in the same way as in the previous measurements of $\alpha_s(M_{Z^0})$ [10], by varying details of the analysis procedure. For each variation, we determine the resulting change in the fitted parameters with respect to the standard result. The uncertainties may be grouped as follows:

Statistical uncertainties: Statistical fluctuations are estimated by repeating the analysis in ten statistically independent subsets of the data and Monte Carlo event samples. Then variances and covariances are computed and the square roots of the variances scaled by $1/\sqrt{10}$ are quoted as the statistical uncertainties for the full sample.

Experimental systematics: In the standard analysis, the event shape observables are computed using both charged tracks and electromagnetic energy deposits in the calorimeter. Experimental effects are considered by repeating the analysis with data derived from charged tracks only or electromagnetic clusters only. The largest difference between any two of the three results is quoted as the experimental uncertainty. As changes of the event selection criteria we restrict the thrust axis of the event to lie within the barrel of the detector ($|\cos \theta_T| < 0.7$), increase the minimum

6

track multiplicity in the event N_{ch} from 5 to 7 and apply an extra cut on missing momentum $|p_{miss}/E_{vis}| < 0.4$. These procedures follow [10], where definitions of the variables involved may be found. The error due to a variation of the ranges of the observables used in the fits is estimated by varying the fit ranges by ± 2 bins around one end of the range while the other end is kept fixed. The largest variation found is quoted as the error due to the variation of the fit range.

Hadronisation systematics: To estimate these uncertainties, we change the parameter set for our standard Monte Carlo program and, in addition, use different Monte Carlo programs with different underlying hadronisation models. A new hadronisation matrix is computed for each change and used in the fits as described above. Further details of the implementation of these changes can be found in [10]. Our standard Monte Carlo program is JETSET 7.3 with the parton shower option [14,15]. The parameters of JETSET have been tuned to OPAL data [9]. The parameters a and σ_q of the JETSET 7.3 Monte Carlo program controlling the string fragmentation are changed about their tuned values by the errors given in [9]. The larger of the deviations of the fit results observed as each parameter is varied up and down is used as the contribution to the total error. As further changes to the analysis, we also consider the use of the Peterson fragmentation function for heavy quarks [16] in JETSET and a variation of the parameter Q_0 controlling the parton virtuality at which the parton shower in JETSET is terminated. We also investigate the effect of the presence of massive b-quarks by correcting the data to consist only of u-, d-, s- and c-events (udsc) using Monte Carlo. As alternative models we use ARIADNE 3.1 [18] and HERWIG 5.5 [17] with parameters tuned to OPAL data [9,19].

Higher order effects: Here we try to estimate the systematic uncertainties due to the uncomputed higher order terms of the theory. We use different approaches for the $\mathcal{O}(\alpha_s^2)$ calculations and the calculations including NLLA terms. The $\mathcal{O}(\alpha_s^2)$ QCD predictions are found to agree much better with the data if the renormalisation scale factor x_μ (see section 3.1) is allowed to vary in the fits as well [10], so we use such fits to define the central results in the fits for structure constants. We estimate the uncertainty due to the variation of the renormalisation scale factor x_μ by repeating the fits of the $\mathcal{O}(\alpha_s^2)$ calculations with $x_\mu = 1$. We define half the observed deviation with respect to fits with x_μ free as the error. However, the observable B_T is found to yield stable fits for all the systematic checks only when the renormalisation scale factor is kept fixed at $x_\mu = 1$. In [10] it was observed that $\mathcal{O}(\alpha_s^2)$ fits to B_T depended only weakly on x_μ and preferred $x_\mu \sim 1$, in contrast to all the other observables studied. Therefore, in the case of B_T, we use the results with $x_\mu = 1$ as the standard and use half the deviation found with x_μ free as the error. For both types of calculation which include NLLA terms, we estimate the influence of missing higher orders by varying x_μ in the range $0.5 < x_\mu < 2.0$ and by taking the deviations from the result with $x_\mu = 1$ as the (asymmetric) errors.

All contributions mentioned above are added in quadrature to obtain the total errors.

Some of the systematic variations are not used in cases where they have only a negligible influence on the results.

3 Theoretical Considerations

Three different types of fit will be used and different steps have to be taken in order to obtain a full decomposition of the QCD predictions into components proportional to the structure constants. Further details about the QCD predictions can be found in [10] and references therein. Furthermore, the dependence of α_s on the energy scale has to be considered, because the running of α_s from a reference value to a certain energy scale depends on the group structure of the theory as well.

3.1 $\mathcal{O}(\alpha_s^2)$ fits

The fixed order QCD coefficients are defined by the general expression for a normalised differential cross section dR/dy of a generic observable y [8, 20]:

$$\frac{dR}{dy} = \frac{1}{\sigma_{tot}}\frac{d\sigma}{dy} = \frac{dA}{dy}C_F\left(\frac{\alpha_s(\mu)}{2\pi}\right) + \left(\left(2\pi\beta_0\ln(x_\mu{}^2) - \frac{3}{4}C_F\right)2C_F\frac{dA}{dy} + \frac{dB}{dy}\right)\left(\frac{\alpha_s(\mu)}{2\pi}\right)^2.$$

(1)

The functions dA/dy and dB/dy are the $\mathcal{O}(\alpha_s)$ and $\mathcal{O}(\alpha_s^2)$ QCD coefficients[1], respectively, and σ_{tot} is the one loop corrected cross section for the process $\mathrm{e^+e^-} \rightarrow$ hadrons. The renormalisation scale factor x_μ is defined by $\mu = x_\mu M_{\mathrm{Z^0}}$, where $M_{\mathrm{Z^0}}$ is the restmass of the $\mathrm{Z^0}$ boson. The scale factor x_μ expresses the dependence on the energy scale μ at which the theory has been renormalised, while β_0 is defined below.

The $\mathcal{O}(\alpha_s)$ QCD coefficients can be used in the fits without any changes, because they are associated with C_F only. The $\mathcal{O}(\alpha_s^2)$ QCD coefficients can be expressed as a sum of structure constant components according to the following equation, where dB_z/dy stands for the term of the dB/dy-function proportional to a structure constant z [8]:

$$\frac{dB}{dy} = C_F\left(C_F\frac{dB_{C_F}}{dy} + C_A\frac{dB_{C_A}}{dy} + N_f\frac{dB_{N_f}}{dy}\right).$$

(2)

The individual terms of the dB/dy-function can be derived by integrating QCD matrix elements three times with two of the three structure constants set to zero in turn, after taking out the global factor of C_F. This has been performed by running a modified version of the QCD matrix element integration program EVENT [21] based on the matrix elements from [22].

3.2 NLLA fits

Resummed QCD calculations (NLLA) matched with $\mathcal{O}(\alpha_s^2)$ calculations have been used widely to measure $\alpha_s(M_{\mathrm{Z^0}})$ with event shape observables [10, 23–28]. NLLA calculations

---

[1]The same coefficients are called $A(y)$ and $B(y)$ in references [8, 20].

can be used on their own to measure $\alpha_s(M_{Z^0})$ [25]. In this analysis we fit the NLLA calculations to restricted ranges of the observables. The NLLA prediction for the cumulative normalised cross section $R(y) = \int_0^y dR/dy'dy'$ is of the form [11, 12]

$$R_{NLLA}(y) = \left(1 + C_1\hat{\alpha}_s + C_2\hat{\alpha}_s{}^2\right)\exp[Lg_1(\hat{\alpha}_s \cdot L) + g_2(\hat{\alpha}_s \cdot L)] \ . \tag{3}$$

where $L = \ln(1/y)$ and $\hat{\alpha}_s = \alpha_s/(2\pi)$. The functions g_1 and g_2 are known from the NLLA calculations and the coefficients C_1 and C_2 are given in [10] for our observables. Expanding the argument of the exponential in equation (3) in powers of $\hat{\alpha}_s$ gives rise to terms of the form $G_{nm}\hat{\alpha}_s{}^nL^m$ with $1 \le m \le n + 1$.

In [10] it was found that implicit or explicit inclusion of the subleading term $G_{21}\hat{\alpha}_s{}^2L$ in the $\mathcal{O}(\alpha_s^2)$+NLLA prediction improved the quality of the fits substantially. The possibility of including terms of the form $G_{21}\hat{\alpha}_s{}^2L$ into the NLLA predictions will therefore be studied in section 4. See also table 3 of [10] for a compilation of the relevant NLLA terms.

The NLLA QCD predictions do not vanish at the kinematic limits y_{max} of the distributions of event shape observables. In [11] the replacement $L \to L' = \ln(1/y - 1/y_{max} + 1)$ is proposed to force the NLLA calculations to vanish at the kinematic limits and thereby possibly allow an adequate description of a larger range of y.

The analytical formulae for the QCD predictions in the NLLA show explicit dependence on the structure constants, so that a decomposition is straightforward [11, 12]. The coefficients of the first subleading term G_{21} and of the second order non-logarithmic term C_2 are not known analytically and thus we computed them numerically from a fit of the NLLA formulae to the fixed order QCD coefficients (generated using EVENT). The decomposition into terms proportional to the structure constants is done by fitting the integrated distributions of the fixed order coefficients separately for each structure constant [29] in a similar way to [11, 12]. The results are shown in table 2. For the study of the QCD structure constants we cannot use the values for G_{21} and C_2 given in [10] since these are not decomposed into structure constant components. Cross checks are performed by adding the individual results for each observable and comparing them with results from fits to the total distributions and with those used in [10]. The results for G_{21} and C_2 are strongly anticorrelated and fixing one of the NLLA coefficients at the value given in [10] reproduces the other one within one standard deviation in all fits at only slightly increased χ^2/d.o.f.. In section 4 the same values for G_{21} and C_2 as in [10] are used for consistency with our previous measurements of $\alpha_s(M_{Z^0})$ while in section 5 the values belonging to each structure constant given in table 2 are employed.

3.3 $\mathcal{O}(\alpha_s^2)$+NLLA fits

The fixed order and the NLLA calculations can be combined to give a prediction which is valid over a larger range of the observables than for either of them alone and which in principle embodies the most complete knowledge of QCD which is presently available. Different procedures describing how to perform this matching exist [10]. For this study the best combination strategy from a theoretical point of view is the $\ln(R)$-matching scheme, because it includes the C_2 and the G_{21} coefficients implicitly and uses explicitly only

those NLLA terms which are known analytically. It also turned out to be the preferred matching scheme in [10], yielding the best fit results in terms of χ^2/d.o.f. in most cases. We therefore choose to employ $\ln(R)$-matching.

3.4   Running of α_s

In our previous studies, the fits were performed in terms of the QCD parameter $\Lambda_{\overline{\text{MS}}}$, in which case the running of α_s to any energy scale depends on the structure constants through the renormalisation group equation (RGE) (4) with a two-loop β-function and its approximate solution (5):

$$\mu\frac{\partial\alpha_s(\mu)}{\partial\mu} = -2\beta_0\alpha_s^2(\mu) - 2\beta_1\alpha_s^3(\mu) - \mathcal{O}(\alpha_s^4(\mu)) \tag{4}$$

$$\beta_0 = \frac{11C_A - 2N_f}{12\pi} \quad\text{and}\quad \beta_1 = \frac{17C_A{}^2 - 5C_A N_f - 3C_F N_f}{24\pi^2}$$

$$\alpha_s(\mu) = \frac{1}{\beta_0 \ln(\mu^2/\Lambda_{\overline{\text{MS}}}^2)}\left(1 - \frac{\beta_1 \ln(\ln(\mu^2/\Lambda_{\overline{\text{MS}}}^2))}{\beta_0^2 \ln(\mu^2/\Lambda_{\overline{\text{MS}}}^2)}\right) \quad . \tag{5}$$

Note that $\alpha_s(\mu)$ will always depend on the structure constants for a given $\Lambda_{\overline{\text{MS}}}$ through (5) even when $x_\mu = 1$. In this study we choose $\alpha_s(M_{\text{Z}^0})$ to be the fundamental parameter which is varied in the fits. We run $\alpha_s(\mu)$ from there using the exact solution of the RGE with a two-loop β-function:

$$\beta_0 \ln(x_\mu^2) = \frac{1}{\alpha_s(\mu)} - \frac{1}{\alpha_s(M_{\text{Z}^0})} + \frac{\beta_1}{\beta_0}\ln\left(\frac{\alpha_s(\mu)}{\alpha_s(M_{\text{Z}^0})}\cdot\frac{\beta_0 + \beta_1\alpha_s(M_{\text{Z}^0})}{\beta_0 + \beta_1\alpha_s(\mu)}\right). \tag{6}$$

Equation (6) is then solved numerically for $\alpha_s(\mu)$ when $x_\mu \neq 1$. This has the formal advantage that there is no dependence on the structure constants through the running of α_s for fits with $x_\mu = 1$.

4   Measurement of $\alpha_s(M_{\text{Z}^0})$ using NLLA calculations

The NLLA calculations can be fitted to data without being matched to $\mathcal{O}(\alpha_s^2)$ calculations in restricted ranges of small y where $L = \ln(1/y)$ is sufficiently large. In addition, it is of interest to extend the NLLA calculations to include the subleading term $G_{21}\hat{\alpha}_s{}^2 L$ and to change variables from L to L' as mentioned in section 3.2. The fits with L changed to L' are referred to as *modified* fits in the following. In order to decide which kind of fit will be used as a standard, we study all four possible variants of the NLLA calculations.

In figures 1 and 2, curves of the QCD calculations using the fitted value for $\alpha_s(M_{\text{Z}^0})$ are shown for the observables $1 - T$ and B_W. The corresponding plots for M_H and B_T show behaviour similar to those for $1 - T$ and B_W, respectively. Results of these fits for all observables are presented in table 3 showing values for $\alpha_s(M_{\text{Z}^0})$, χ^2/d.o.f. and where appropriate other fit variables. The unchanged NLLA calculations lead to satisfactory

10

fits for $1 - T$ and M_H only. For B_T and B_W, the values of $\chi^2/\text{d.o.f.}$ are much larger. In these cases the fits fail to describe the data in the 2-jet regions (small y) and even in the ranges used for the fits agreement is poor, see figure 2 a). The NLLA+G_{21} fits shown in figures 1 b) and 2 b) result in reasonable $\chi^2/\text{d.o.f.}$ for all observables and the data in the 2-jet region are well described. The great importance of the $G_{21}\hat{\alpha}_s{}^2 L$ term in the fits with B_T and B_W presumably stems from the large numerical values of G_{21} for these observables [10]. The modified NLLA fits also provide satisfactory fits for all variables, as seen from table 3, suggesting that the modification might simulate the inclusion of the subleading terms in the calculations. It is seen, however, from figures 1 c) and 2 c), that the modified NLLA predictions lie below the data at large y. The description of the peaks at small y by the modified NLLA calculations is slightly worse than by the NLLA+G_{21} calculations. The combination of both changes to the NLLA predictions, the modified NLLA+G_{21} fits shown in figures 1 d) and 2 d), yield a significantly worse agreement with the data especially at the peaks at small y. In conclusion, we choose the NLLA+G_{21} fits as the standard method for this part of the analysis, because they provide the most consistent description of the data.

In figures 3 a) to d) the dependence of $\chi^2/\text{d.o.f.}$ and $\alpha_s(M_{Z^0})$ on the renormalisation scale parameter x_μ is shown for the NLLA+G_{21} fits. With the NLLA+G_{21} calculations, the minima of χ^2 are well defined and clearly prefer values of x_μ of about unity for all four observables.

As variations of the analysis, fits with the renormalisation scale, x_μ, or with the lowest order uncomputed NLLA coefficient, G_{32}, as additional free parameters are performed. The results are given in table 3. For the standard NLLA+G_{21} fits, the values for x_μ are found to be of $\mathcal{O}(1)$ with small changes to the fitted values for $\alpha_s(M_{Z^0})$ relative to their values with $x_\mu = 1$ kept fixed. It is theoretically expected that NLLA calculations should not lead to values of x_μ significantly different from unity in fits, if higher order terms are correctly accounted for [11,12]. In the case of the NLLA fits the values for x_μ turn out to be smaller, having values of 0.11 for B_T and B_W, implying the presence of significant missing higher order terms.

In fits with the NLLA coefficient G_{32} as a free parameter, a term $G_{32}\hat{\alpha}_s{}^3 L^2$ which is of $\mathcal{O}(\alpha_s^3)$ is included in the calculation. These fits test the importance of missing higher orders in the NLLA+G_{21} prediction. It is found that the values of $\alpha_s(M_{Z^0})$ obtained in the fits do not change significantly when G_{32} is allowed to vary. The values for G_{32} are consistent with zero for all observables except B_W. Since the influence on the fitted values of $\alpha_s(M_{Z^0})$ is negligible, and the influence of higher orders is already estimated by varying x_μ, we do not include this systematic check in the estimate of the total errors.

The results of the systematic variations of the NLLA analysis are summarised in table 4. The total hadronisation uncertainties are larger compared to the $\mathcal{O}(\alpha_s^2)$ and the $\mathcal{O}(\alpha_s^2)$+NLLA fits [10], because the fits include regions of y where these corrections are quite large and more dependent on the model used. The scale uncertainties of the NLLA fits are comparable to scale uncertainties with $\mathcal{O}(\alpha_s^2)$+NLLA fits. The errors due to variations of the fit ranges turn out to be negligible. The total accuracy of the measurements of $\alpha_s(M_{Z^0})$ is about 10%, and is thus comparable to the accuracy achieved

11

using the $\mathcal{O}(\alpha_s^2)$ or $\mathcal{O}(\alpha_s^2)$+NLLA calculations.

To obtain a single result for $\alpha_s(M_{Z^0})$, the four individual results are combined by computing an error weighted average following the same procedure as [10]. The total errors given in table 4 are used as the weights. In order to estimate the total error of the combined result, the weighted average is computed with the individual results from each systematic variation of the analysis using the same weights throughout. The final result is

$$\alpha_s(M_{Z^0}) = 0.113^{+0.009}_{-0.008} \quad .$$

As a cross check, a simultaneous fit to all four observables is performed, yielding $\alpha_s(M_{Z^0}) = 0.113 \pm 0.009$ with $\chi^2/\text{d.o.f.} = 9.8$. The final result is lower than but still consistent with the OPAL measurement $\alpha_s(M_{Z^0}) = 0.120 \pm 0.006$ based on $\mathcal{O}(\alpha_s^2)$+NLLA calculations with seven event shape observables [10]. We regard the result from [10] as our best estimate of $\alpha_s(M_{Z^0})$ since it is based on the most complete calculations with a more comprehensive set of observables and has smaller errors.

The results of this analysis are compared in figure 4 with results taken from [10] for the same four observables from fits using $\mathcal{O}(\alpha_s^2)$ and $\mathcal{O}(\alpha_s^2)$+NLLA calculations based on the same data sample. The vertical lines and shaded bands indicate the combined results obtained by the weighted average for each type of fit. In the case of $\mathcal{O}(\alpha_s^2)$ fits, individual results from fits with $x_\mu = 1$ (squares) and x_μ free (triangles) are also shown. The $\mathcal{O}(\alpha_s^2)$ fits yield somewhat larger results for $\alpha_s(M_{Z^0})$ than the fits including NLLA terms, but it must be remembered that the $\mathcal{O}(\alpha_s^2)$ results are the average between fits with varied renormalisation scale and fixed renormalisation scale [10]. Thus the effective values of x_μ corresponding to the quoted results are not those which lead to the best fits. The results from $\mathcal{O}(\alpha_s^2)$ fits with x_μ free lie closer to the results from the other types of fit in all cases. In conclusion, after considering the total errors, the results from the three types of fit agree with each other, indicating consistency between the three different QCD calculations. The NLLA+G_{21} results appear to be systematically lower than the results including $\mathcal{O}(\alpha_s^2)$ terms, but are compatible within the errors.

5 Results of fits to QCD structure constants

We now present results of the fits in which $\alpha_s(M_{Z^0})$ and one of the structure constants C_A, C_F or N_f are varied. A simultaneous determination of pairs of structure constants in conjunction with $\alpha_s(M_{Z^0})$ proved to result in unstable fits, indicating that sensitivity to the structure constants is limited. Therefore, in our fits, only one of the structure constants is allowed to vary at a time, while the others are fixed to their standard QCD values. In the fits using the $\mathcal{O}(\alpha_s^2)$ calculations, the renormalisation scale factor x_μ is also allowed to vary. In addition to fitting each observable separately, we also perform combined fits of the theory to all four observables simultaneously, in which a common value of $\alpha_s(M_{Z^0})$ and one structure constant are allowed to vary. Correlations between different observables are neglected. In the combined fits with the $\mathcal{O}(\alpha_s^2)$ calculations, renormalisation scale factors $x_\mu^{(y)}$ are allowed to vary for each observable y separately.

The results of the standard fits are given in tables 5, 6 and 7 together with statistical errors and the systematic deviations with respect to the standard results. The values of $\alpha_s(M_{Z^0})$ and $\chi^2/\text{d.o.f.}$ found in the central fits are also given in these tables. In the case of the $\mathcal{O}(\alpha_s^2)$ fits, we also list the fitted values for x_μ for the central fits. The fit results for the structure constants are summarised in figure 5. The results for N_f and C_A are presented in terms of the ratios T_F/C_F and C_A/C_F to allow a comparison with the OPAL results published in [7]. These results are indicated by the shaded bands while the dashed lines show the expectation from QCD. Results for $\alpha_s(M_{Z^0})$ from the same fits are shown in figure 6 with total errors including all systematic effects considered in this study. The dashed lines and shaded areas indicate the corresponding measurements of $\alpha_s(M_{Z^0})$ and their uncertainties from figure 4.

5.1 Fit quality

5.1.1 $\mathcal{O}(\alpha_s^2)$ fits

The results of the $\mathcal{O}(\alpha_s^2)$ fits are summarised in table 5. In the case of fits with B_T, the renormalisation scale factor is kept fixed at $x_\mu = 1$ as explained above. The $\chi^2/\text{d.o.f.}$ values of the fits are of the order of unity. The values for x_μ are consistent with values found previously [10]. The structure constants are in better agreement with QCD and the $\chi^2/\text{d.o.f.}$ of the fits are smaller if x_μ is allowed to vary than if it is not. The biggest contributions to the errors typically arise from the variation of the renormalisation scale factor x_μ and the variation of the fit ranges. The total errors turn out to be large, so that the structure constants are not well measured using the $\mathcal{O}(\alpha_s^2)$ fits.

5.1.2 NLLA fits

Using the NLLA+G_{21} calculation, we obtain the results summarised in table 6. The uncertainties stemming from the hadronisation correction are the main contributions to the total errors. Only restricted ranges of small y are fitted where the hadronisation corrections are large and less well known. The total errors are large, with the result that the structure constants are also poorly determined for this class of calculations.

5.1.3 $\mathcal{O}(\alpha_s^2)$+NLLA fits

The results found using the $\mathcal{O}(\alpha_s^2)$+NLLA calculations are summarised in table 7. The main contributions to the total errors are generally the experimental uncertainties, the hadronisation correction, the effects of using a different renormalisation scale x_μ and the variation of the ranges used in the fits. The total errors which result from these fits are significantly smaller than those found with the other two types of QCD calculation, however. The precision is not much different from that obtained from the OPAL analysis of 4-jet events [7], as seen from figure 5.

5.1.4 Combined Fits

The combined fits to all four observables lead to an improvement in the total errors for the $\mathcal{O}(\alpha_s^2)$+NLLA calculations only. With the other two types of calculations, the results are consistent with those from the individual fits, but the total errors do not improve. The value of χ^2/d.o.f. for the combined fit is larger than the values of χ^2/d.o.f. for the individual fits, using the $\mathcal{O}(\alpha_s^2)$+NLLA or NLLA+G_{21} calculations. If B_W is not included in the combined fits, the values of χ^2/d.o.f. decrease significantly to χ^2/d.o.f. $\simeq 4.5$ ($\mathcal{O}(\alpha_s^2)$+NLLA) or χ^2/d.o.f. $\simeq 2.5$ (NLLA+G_{21}).

5.2 Fit results

5.2.1 Fits to C_A

From tables 5, 6 and 7 it is seen that the values for C_A are consistent with $C_A = 3$ within one standard deviation of the total error for all observables used in the fits and for all three types of QCD calculation.

5.2.2 Fits to C_F

Fits to C_F and $\alpha_s(M_{Z^0})$ with all three types of QCD calculations yield values for C_F which are consistent with $C_F = \frac{4}{3}$ to within one or two standard deviations of the total error. With the $\mathcal{O}(\alpha_s^2)$+NLLA calculations, the values of χ^2/d.o.f. for fits with B_W are lower than for fits to $\alpha_s(M_{Z^0})$ only [10]. The χ^2/d.o.f. is reduced from 18.8 to 0.4 and the value for $\alpha_s(M_{Z^0})$ is significantly larger than previously. The same effect is seen in the NLLA fits.

5.2.3 Fits to N_f

With the $\mathcal{O}(\alpha_s^2)$+NLLA fits to N_f and $\alpha_s(M_{Z^0})$, three of the four observables show a reasonable sensitivity to the structure constant as seen from table 7. In the case of B_W the fits do not converge to minima of χ^2 inside the bounds of the fitted parameters[2]. Similarly, the fits with M_H using HERWIG and with B_T corrected for b-quark mass effects fail to converge to a minimum of χ^2. We therefore cannot quote errors due to these effects. The total errors given for M_H and B_T should, as a consequence, be considered as lower limits to the true errors.

The NLLA+G_{21} QCD predictions also give stable fits to N_f and $\alpha_s(M_{Z^0})$ for all observables except B_W, as listed in table 6. These fits suffer from the large effects of the variations of the hadronisation model. The fit to the B_T-distribution corrected for b-quark mass effects fails to converge and the total error is calculated without this contribution.

When the $\mathcal{O}(\alpha_s^2)$ QCD predictions are used, we find stable fits for all observables except $1 - T$, where the fit does not converge inside the bounds imposed on N_f; see table 5.

---

[2]The bounds are $0.01 < \alpha_s(M_{Z^0}) < 1.0$, $0 < N_f < 20$, $0 < C_A < 10$ and $0 < C_F < 10$.

5.3 Correlation plots

The choice of a particular gauge group for QCD determines the set of structure constants, as mentioned in the introduction. A comparison of the expectations for some reasonable choices of the underlying group with measurements of the structure constants can be done in two dimensional planes spanned by pairs of structure constants. The analyses of 4-jet events led to simultaneous measurements of the structure constant ratios T_F/C_F and C_A/C_F and results were compared in a T_F/C_F–C_A/C_F plane [4–7]. In the present study, we fit for only one structure constant at a time. The results for any pair of structure constants for a given data sample may still be correlated, however. These correlations can be determined using standard statistical techniques. Error ellipses for a pair of structure constants can then be drawn using the individual results, the total errors on each structure constant and the correlation coefficient ρ. In order to account for the fact that the pair of structure constants is not measured simultaneously, the errors are multiplied by $1/\sqrt{1-\rho^2}$ and the centre of the error ellipse is shifted to the most likely position of a combined measurement using the formulae given in [30]. We are thus also able to display our results in a T_F/C_F–C_A/C_F plane. In addition, we present a comparison in a C_F–C_A/C_F plane, which allows a test of the constraint $C_F = (C_A{}^2 - 1)/(2C_A)$ when considering gauge groups of the SU(N) type.

We use results based on the $\mathcal{O}(\alpha_s^2)$+NLLA fits to all four observables simultaneously, because these provided the most stable and precise results, and also because such calculations incorporate the most complete theoretical knowledge. We draw the error ellipses based on correlation coefficients between the structure constants and the total errors for each structure constant as quoted in table 7. We compute the statistical covariances between each pair of structure constants by repeating the analysis on ten statistically independent subsets of the corrected data.

The inclusion of systematic uncertainties into the covariance matrices is done as follows. We add all systematic uncertainties apart from the uncertainties due to the variation of x_μ, experimental effects and the variation of the fit range to the statistical covariance matrix treating them as fully correlated. However, since the variation of x_μ is believed to partly absorb higher order effects, there is no reason why the preferred value of x_μ should be the same for all fits. We also conservatively assume the uncertainties from experimental effects and the fit ranges to be uncorrelated. We therefore add the errors due to x_μ, experimental effects and the fit range in quadrature to the diagonal elements of the covariance matrix. Then the correlation coefficients are computed. We find that the statistical correlations are $\rho(T_F, C_A) = -0.998$ and $\rho(C_F, C_A) = -0.996$. After systematic uncertainties are taken into account as described above, we find $\rho(T_F, C_A) = -0.72$ and $\rho(C_F, C_A) = -0.68$.

The resulting error ellipses for one, two and three standard deviations are shown in figure 7. The error ellipses correspond to confidence levels of 39%, 86% and 99%, respectively. In the T_F/C_F–C_A/C_F plane (figure 7 a)) the possibility of the Abelian gluon model with U(1)$_3$ as the underlying group ($T_F/C_F = 3$, $C_A/C_F = 0$) can be excluded at more than 99% confidence level. The prediction of QCD with the additional presence of

15

one light gluino [31,32] is shown in the approximation that the gluino is massless, which corresponds to an effective $N_f = 8$ and $C_A/C_F = 2.25$. This scenario seems less likely than standard QCD but cannot be reliably excluded. Similar conclusions were reached in [7] based on an analysis of 4-jet events whose results are shown as a shaded one standard deviation contour on figure 7 a). In the C_F–C_A/C_F plane (figure 7 b)) the Abelian gluon model ($C_F = 1$, $C_A/C_F = 0$) is excluded with a confidence level of more than 99%. The position of the SU(N) constraint is indicated by the dashed-dotted line on the plot.

6   Summary and conclusions

Fits of QCD predictions of event shape cross sections for the observables $1 - T$, M_H, B_T and B_W are described. We present a determination of the strong coupling $\alpha_s(M_{Z^0})$ based on NLLA calculations, and an analysis of the QCD structure constants C_A, N_f (T_F) and C_F employing three different types of QCD calculation: $\mathcal{O}(\alpha_s^2)$, NLLA and $\mathcal{O}(\alpha_s^2)$+NLLA calculations. The structure constant analysis described here is based on the sensitivity of higher order corrections to the 3-jet cross section to the gauge structure of QCD and may be considered as complementary to the 4-jet analyses [5–7]. The calculations including resummed NLLA terms are valid beyond tree level, unlike the 4-jet analyses of QCD structure constants.

The NLLA calculations allow a measurement of $\alpha_s(M_{Z^0})$ using regions of the distributions at small y. The fits are found to be satisfactory for all four observables once the subleading term $G_{21}\hat{\alpha_s}^2 L$ is included in the predictions. The results for $\alpha_s(M_{Z^0})$ are systematically smaller than but compatible with results from $\mathcal{O}(\alpha_s^2)$ or $\mathcal{O}(\alpha_s^2)$+NLLA fits [10] and the total errors are only slightly larger. This indicates that the NLLA+G_{21} calculations provide an adequate description of the data in restricted regions of y mainly populated by 2-jet events without hard gluon radiation.

We find all results for the QCD structure constants to be in agreement with standard QCD based on SU(3) and five active quark flavours within one or two standard deviations of the total errors. The values for $\alpha_s(M_{Z^0})$ from our fits are compatible with previous measurements. However it is only with the $\mathcal{O}(\alpha_s^2)$+NLLA fits that the numerical values of the structure constants are reasonably well determined. The possibility of QCD without the triple gluon vertex (TGV) can be excluded safely using the fit of $\mathcal{O}(\alpha_s^2)$+NLLA ($\ln(R)$-matching) predictions to all observables simultaneously. Based on the combined $\mathcal{O}(\alpha_s^2)$+NLLA fits with all four observables, the possibility of the presence of a massless light gluino seems less likely than standard QCD without any extra fermionic contributions, but cannot be excluded.

The $\mathcal{O}(\alpha_s^2)$ calculations give satisfactory fits when the renormalisation scale factor x_μ is allowed to vary for each observable. The values found for x_μ in our fits are similar to those found previously in measurements of $\alpha_s(M_{Z^0})$. This observation gives confidence in the interpretation that the small values of x_μ account for missing higher order terms in a consistent way, because the structure constants are in better agreement with QCD when the renormalisation scale factor is not fixed to $x_\mu = 1$ but is allowed to vary in the fits.

16

The total errors on the measurements of C_A/C_F and T_F/C_F are larger than the errors obtained in the 4-jet analyses [5–7] but still allow a reasonable measurement of the structure constants, at least by using the $\mathcal{O}(\alpha_s^2)$+NLLA QCD calculations. However, it should be emphasized that the present results include uncertainties due to higher order contributions through variations of the renormalisation scale, which could not be estimated in the case of the 4-jet analyses. In addition, we consider extra hadronisation effects which could not readily be estimated in the 4-jet analyses.

Acknowledgements

References

[1] T. Muta: Foundations of quantum chromo dynamics. Vol. 5 of World Scientific Lecture Notes in Physics, World Scientific 1987

[2] M.Z. Akrawy et al., OPAL Coll.: Z. Phys. C 49 (1991) 49

[3] B. Adeva et al., L3 Coll.: Phys. Lett. B 248 (1990) 227

[4] P. Abreu et al., DELPHI Coll.: Phys. Lett. B 255 (1991) 466

17

[5] P. Abreu et al., DELPHI Coll.: Z. Phys. C 59 (1993) 357

[6] D. Decamp et al., ALEPH Coll.: Phys. Lett. B 284 (1992) 151

[7] R. Akers et al., OPAL Coll.: Z. Phys. C 65 (1995) 367

[8] N. Magnoli, P. Nason and R. Rattazzi: Phys. Lett. B 252 (1990) 271

[9] M.Z. Akrawy et al., OPAL Coll.: Z. Phys. C 47 (1990) 505

[10] P.D. Acton et al., OPAL Coll.: Z. Phys. C 59 (1993) 1

[11] S. Catani, L. Trentadue, G. Turnock and B.R. Webber: Nucl. Phys. B 407 (1993) 3

[12] S. Catani, G. Turnock and B.R. Webber: Phys. Lett. B 295 (1992) 269

[13] K. Ahmet et al., OPAL Coll.: Nucl. Instrum. Methods A 305 (1991) 275

[14] T. Sjöstrand: Comput. Phys. Commun. 39 (1986) 347

[15] T. Sjöstrand and M. Bengtson: Comput. Phys. Commun. 43 (1987) 367

[16] C. Peterson, D. Schlatter, I. Schmitt and P. Zerwas: Phys. Rev. D 27 (1983) 105

[17] G. Marchesini et al.: Comput. Phys. Commun. 67 (1992) 465

[18] L. Lönnblad: Comput. Phys. Commun. 71 (1992) 15

[19] P.D. Acton et al., OPAL Coll.: Z. Phys. C 58 (1993) 387

[20] Z. Kunszt and P. Nason [conv.]: In: Z physics at LEP 1, G.Altarelli, R.Kleiss and C.Verzegnassi (eds.), Vol. 1, CERN 89-08 1989

[21] P. Nason: private communication

[22] R.K. Ellis, D.A. Ross and A.E. Terrano: Nucl. Phys. B 178 (1981) 421

[23] P.D. Acton et al., OPAL Coll.: Z. Phys. C 55 (1992) 1

[24] D. Decamp et al., ALEPH Coll.: Phys. Lett. B 284 (1992) 163

[25] P. Abreu et al., DELPHI Coll.: Z. Phys. C 59 (1993) 21

[26] O. Adriani et al., L3 Coll.: Phys. Lett. B 284 (1992) 471

[27] Y. Ohnishi et al., TOPAZ Coll.: Phys. Lett. B 313 (1993) 475

[28] K. Abe et al., SLD Coll.: Phys. Rev. D 51 (1995) 962

[29] S. Kluth: Ph.D. thesis, Cambridge University, 1994

[30] L. Lyons: Statistics for nuclear and particle physics. Cambridge University Press 1986, page 60

[31] M. Jezabek and J.H. Kühn: Phys. Lett. B 301 (1993) 121

[32] J. Ellis, D.V. Nanopoulos and D.A. Ross: Phys. Lett. B 305 (1993) 375

Tables

	$\mathcal{O}(\alpha_s^2)$	$\mathcal{O}(\alpha_s^2)$+NLLA	NLLA	$L = \ln(1/y)$
$1 - T$	$0.13 - 0.32$	$0.11 - 0.32$	$0.06 - 0.17$	2.81–1.77
M_H	$0.26 - 0.54$	$0.20 - 0.40$	$0.18 - 0.28$	3.43–2.54
B_T	$0.15 - 0.29$	$0.10 - 0.24$	$0.09 - 0.16$	2.41–1.83
B_W	$0.09 - 0.23$	$0.08 - 0.16$	$0.05 - 0.12$	3.00–2.12

Table 1: Ranges of the event shape distributions used in the fits. For NLLA the ranges are also shown in $L = \ln(1/y)$.

		$1 - T$	M_H	B_T	B_W
C_F	G_{21}	7 ± 3	7 ± 2	185 ± 10	189 ± 4
	C_2	32 ± 9	22 ± 6	-198 ± 31	-247 ± 13
C_A	G_{21}	43 ± 6	46 ± 6	75 ± 9	74 ± 8
	C_2	-3 ± 19	6 ± 19	8 ± 27	36 ± 25
N_f	G_{21}	-20.0 ± 0.4	-19.2 ± 0.4	-32.3 ± 0.6	-31.9 ± 0.6
	C_2	6 ± 1	8 ± 1	-4 ± 2	0 ± 2
Σ	G_{21}	29 ± 7	34 ± 7	226 ± 14	233 ± 9
	C_2	37 ± 21	38 ± 20	-187 ± 41	-217 ± 29

Table 2: Values of G_{21} and C_2 from fits to fixed order QCD coefficients. In the rows labelled Σ the fits are done with the sum of the three terms of the $\mathcal{O}(\alpha_s^2)$ QCD coefficients.

		$1-T$	M_H	B_T	B_W
NLLA	$\alpha_s(M_{Z^0})$	0.1152	0.1170	0.1208	0.1136
	χ^2/d.o.f.	6.3	6	61	186
NLLA+G_{21}	$\alpha_s(M_{Z^0})$	**0.1152**	**0.1150**	**0.1146**	**0.1088**
	$\Lambda_{\overline{\mathrm{MS}}}$ [MeV]	193 ± 5	191 ± 4	185 ± 5	129 ± 3
	χ^2/d.o.f.	3.2	0.9	2	12.5
modified NLLA	$\alpha_s(M_{Z^0})$	0.1113	0.1113	0.1079	0.1013
	χ^2/d.o.f.	3	4.3	2.7	28
modified NLLA+G_{21}	$\alpha_s(M_{Z^0})$	0.1115	0.1100	0.1046	0.0976
	χ^2/d.o.f.	2.2	1.8	22	7.3
NLLA	$\alpha_s(M_{Z^0})$	0.1089	0.1112	0.1014	0.1009
x_μ fitted	x_μ	0.41	0.53	0.11	0.11
	χ^2/d.o.f.	3.7	1.3	2.2	4.2
NLLA+G_{21}	$\alpha_s(M_{Z^0})$	0.1132	0.1146	0.1141	0.1027
x_μ fitted	x_μ	0.78	0.96	0.96	0.52
	χ^2/d.o.f.	3.3	1.1	2.4	5.2
NLLA+G_{21}	$\alpha_s(M_{Z^0})$	0.1160	0.1151	0.1146	0.1088
G_{32} fitted	G_{32}	240 ± 150	60 ± 150	100 ± 350	1830 ± 260
	χ^2/d.o.f.	3.3	1.1	2.4	5

Table 3: Values of $\alpha_s(M_{Z^0})$, χ^2/d.o.f. and where appropriate other fitted variables derived by fitting NLLA QCD calculations to data. In the first four fits, the renormalisation scale factor is set to $x_\mu = 1$ and $G_{32} = 0$. In the next two fits x_μ is varied and in the final fit G_{32} is determined in the fits.

	$1-T$	M_H	B_T	B_W
$\alpha_s(M_{Z^0})$	**0.1152**	**0.1150**	**0.1146**	**0.1088**
Statistical	± 0.0006	± 0.0003	± 0.0005	± 0.0003
tracks only	$+0.0007$	$+0.0009$	$+0.0014$	$+0.0012$
cluster only	-0.0017	-0.0006	-0.0022	-0.0015
$\|\cos\theta_T\| < 0.7$	0.0000	$+0.0004$	$+0.0001$	$+0.0003$
$N_{ch} \geq 7$	$+0.0002$	$+0.0002$	$+0.0002$	$+0.0002$
$\|p_{miss}/E_{vis}\| < 0.4$	$+0.0001$	$+0.0001$	0.0000	0.0000
Experimental Syst.	± 0.0024	± 0.0015	± 0.0036	± 0.0027
$a + 1$ s.d.	-0.0014	-0.0033	-0.0021	-0.0012
$a - 1$ s.d.	$+0.0008$	$+0.0015$	$+0.0010$	$+0.0007$
$\sigma_q + 1$ s.d.	-0.0010	-0.0009	-0.0010	-0.0008
$\sigma_q - 1$ s.d.	$+0.0017$	$+0.0017$	$+0.0017$	$+0.0015$
Peterson	$+0.0001$	$+0.0009$	-0.0024	-0.0018
udsc only	$+0.0027$	0.0000	$+0.0058$	$+0.0044$
$Q_0 = 2$ GeV	-0.0010	-0.0005	-0.0021	$+0.0003$
Herwig 5.5	-0.0034	$+0.0112$	-0.0091	-0.0016
Ariadne 3.1	-0.0001	$+0.0004$	-0.0036	-0.0003
Total Hadronisation	± 0.0050	± 0.0119	± 0.0121	± 0.0055
$x_\mu = 0.5$	-0.0052	-0.0061	-0.0076	-0.0065
$x_\mu = 2$	$+0.0063$	$+0.0072$	$+0.0090$	$+0.0075$
Total error	**+0.0084** **−0.0076**	**+0.0140** **−0.0135**	**+0.0155** **−0.0147**	**+0.0097** **−0.0089**

Table 4: Errors on the value of $\alpha_s(M_{Z^0})$ derived using NLLA+G_{21} QCD calculations with $x_\mu = 1$. Where a signed value is quoted, this indicates the direction in which $\alpha_s(M_{Z^0})$ changed with respect to the default analysis when a certain feature of the analysis is changed. A detailed description of these systematic studies is given in [10].

	$\mathcal{O}(\alpha_s^2)$ fits to C_A					$\mathcal{O}(\alpha_s^2)$ fits to C_F					$\mathcal{O}(\alpha_s^2)$ fits to N_f			
	$1-T$	M_H	B_T	B_W	all	$1-T$	M_H	B_T	B_W	all	M_H	B_T	B_W	all
central	**4.0**	**2.9**	**2.7**	**3.2**	**3.0**	**0.9**	**1.4**	**2.8**	**1.2**	**1.4**	**5.8**	**4.9**	**3.7**	**3.4**
$\alpha_s(M_{Z^0})$	0.096	0.119	0.142	0.113	0.118	0.145	0.113	0.073	0.122	0.115	0.120	0.139	0.111	0.109
$\Delta\alpha_s(M_{Z^0})$	±.063	±.023	±.046	±.013	±.040	±.095	±.066	±.086	±.035	±.014	±.044	±.013	±.024	±.030
x_μ	0.08	0.06	1.0	0.07	–	0.10	0.06	1.0	0.07	–	0.06	1.0	0.07	–
χ^2/d.o.f.	1.9	1.8	2.9	0.6	3.5	1.9	1.8	2.3	0.6	3.4	1.9	3	0.6	3.3
stat.	±1.0	±0.1	±0.4	±0.1	±0.1	±0.2	±0.1	±1.2	±0.1	±0.0	±0.8	±0.7	±0.7	±0.8
expt.	±0.8	±0.3	±0.3	±0.2	±0.2	±0.3	±0.2	±0.7	±0.1	±0.1	±3.1	±0.7	±1.4	±1.9
Fit range	±1.0	±0.1	±2.1	±0.1	±2.7	±0.4	±0.1	±1.3	±0.1	±0.4	±0.9	±2.2	±1.1	±1.3
$a+1$ st.d.	−1.3	±0.0	+0.1	±0.0	±0.0	+0.6	±0.0	+1.3	±0.0	±0.0	−0.6	−0.6	+0.2	−0.1
$a-1$ st.d.	−0.2	+0.4	+0.6	+0.2	+0.2	+0.1	−0.2	−0.4	−0.1	±0.0	−3.4	−1.3	−1.4	−2.6
σ_q+1 st.d.	−0.7	+0.3	+0.1	+0.1	+0.1	+0.3	−0.1	+0.1	−0.1	±0.0	−2.3	−0.3	−0.9	−1.1
σ_q-1 st.d.	±0.0	+0.4	+0.4	+0.2	+0.1	±0.0	−0.2	+0.6	−0.1	±0.0	−3.1	−1.3	−1.3	−2.5
Peterson	−0.8	+0.3	−0.3	+0.1	+0.1	+0.3	−0.1	−0.7	−0.1	±0.0	−2.5	+0.5	−0.8	−1.0
udsc quarks	−0.6	+0.4	+1.1	+0.2	+0.1	+0.3	−0.2	+0.2	−0.1	±0.0	−2.7	−2.3	−1.7	−2.8
$Q_0 = 6$ GeV	−1.5	−0.1	−0.5	−0.1	±0.0	+0.8	+0.1	+7.2	+0.1	±0.0	−0.5	+0.4	+0.7	+0.9
HERWIG 5.5	−0.9	+0.4	−0.8	+0.2	+0.2	+0.3	−0.2	+3.4	−0.1	−0.1	−4.4	+1.7	−1.2	+0.3
ARIADNE 3.1	−0.9	+0.2	−0.5	±0.0	±0.0	+0.4	−0.1	+5.0	±0.0	±0.0	−1.9	+0.8	+0.3	+0.5
$x_\mu = 1.0$	−3.2	+2.8	–	+0.9	−0.5	−0.3	−0.8	–	−0.4	±0.0	+9.0	–	+5.4	+6.4
x_μ free	–	–	+0.9	–	–	–	–	±0.0	–	–	–	+0.2	–	–
Total error	**±3.1**	**±1.7**	**±2.8**	**±0.7**	**±2.7**	**±1.4**	**±0.6**	**±9.7**	**±0.3**	**±0.4**	**±8.9**	**±4.3**	**±4.1**	**±5.3**

Table 5: Results of fits using the $\mathcal{O}(\alpha_s^2)$ calculations. One of the three structure constants, $\alpha_s(M_{Z^0})$ and the renormalisation scale factor x_μ are allowed to vary in the fits while the other two structure constants are kept fixed at their standard values. In the case of fits with B_T the central results are obtained with $x_\mu = 1$ fixed. Errors on the structure constants are given as deviations from the central results. In the case of fits to N_f and $\alpha_s(M_{Z^0})$ with $1-T$ the fits failed to converge and no results are quoted.

	NLLA+G_{21} fits to C_A					NLLA+G_{21} fits to C_F					NLLA+G_{21} fits to N_f			
	$1-T$	M_H	B_T	B_W	all	$1-T$	M_H	B_T	B_W	all	$1-T$	M_H	B_T	all
central	**3.1**	**3.0**	**3.0**	**3.6**	**3.0**	**1.3**	**1.3**	**1.3**	**1.0**	**1.3**	**4.5**	**4.7**	**5.0**	**4.7**
$\alpha_s(M_{Z^0})$	0.113	0.114	0.116	0.094	0.113	0.118	0.117	0.116	0.122	0.115	0.113	0.114	0.116	0.113
$\Delta\alpha_s(M_{Z^0})$	±.030	±.026	±.079	±.025	±.041	±.068	±.028	±.104	±.038	±.061	±.030	±.028	±.076	±.046
χ^2/d.o.f.	3.4	1.1	2.1	4.8	9.7	3.4	1.1	1.4	5.0	9.8	3.4	1.1	2.1	9.7
stat.	±0.1	±0.1	±0.1	±0.1	±0.1	±0.1	±0.0	±0.1	±0.0	±0.0	±0.4	±0.4	±0.7	±0.3
expt.	±0.0	±0.2	±0.2	±0.1	±0.0	±0.0	±0.1	±0.1	±0.0	±0.0	±0.2	±1.2	±0.8	±0.1
Fit range	±0.5	±0.3	±0.5	±0.7	±0.2	±0.3	±0.2	±0.3	±0.2	±0.2	±2.8	±1.7	±2.8	±1.7
$a+1$ st.d.	−0.2	−0.5	−0.4	−0.3	−0.3	+0.1	+0.4	+0.3	+0.1	+0.2	+0.8	+2.6	+1.9	+1.6
$a-1$ st.d.	+0.1	+0.2	+0.1	+0.1	+0.1	−0.1	−0.1	−0.1	+0.0	−0.1	−0.8	−1.2	−0.7	−0.8
σ_q+1 st.d.	−0.1	−0.2	−0.1	−0.1	−0.1	+0.0	+0.1	+0.1	+0.0	+0.1	+0.4	+0.9	+0.7	+0.5
σ_q-1 st.d.	+0.2	+0.2	+0.2	+0.2	+0.2	−0.1	−0.1	−0.1	−0.1	−0.1	−1.2	−1.2	−1.2	−1.0
Peterson	+0.0	−0.1	−0.7	−0.5	−0.2	+0.0	+0.0	+0.7	+0.2	+0.2	+0.0	+0.3	+3.7	+1.3
udsc quarks	+0.3	+0.0	+0.7	+0.6	+0.2	−0.2	+0.0	−0.3	−0.2	−0.1	−1.5	+0.3	−4.0	−1.1
$Q_0=2$ GeV	−0.1	−0.2	−0.3	+0.0	+0.1	+0.0	+0.1	+0.2	+0.0	+0.0	+0.3	+1.2	+1.4	+0.4
HERWIG 5.5	−1.3	+0.0	−1.7	−0.7	−1.3	+2.2	+0.0	+8.7	+0.4	+2.0	+6.6	+0.0	+8.1	+7.0
ARIADNE 3.1	−0.1	−0.5	−0.6	−0.4	−0.4	+0.1	+0.4	+0.6	+0.2	+0.3	+0.6	+2.9	+3.3	+2.0
$x_\mu=0.5$	−0.3	−0.4	−0.4	−0.7	−0.4	+0.2	+0.3	+0.4	+0.3	+0.3	+1.7	+2.0	+2.4	+2.4
$x_\mu=2.0$	+0.3	+0.4	+0.5	+0.8	+0.5	−0.2	−0.2	−0.3	−0.2	−0.2	−1.9	−2.2	−2.8	−2.6
Total error	**±1.5**	**±0.9**	**±2.3**	**±1.6**	**±1.5**	**±2.2**	$^{+0.6}_{-0.7}$	**±8.7**	**±0.6**	**±2.0**	**±7.6**	**±11**	**±12**	**±8.3**

Table 6: Results of fits using NLLA+G_{21} calculations. One of the three structure constants and $\alpha_s(M_{Z^0})$ are allowed to vary in the fits while the other two structure constants are kept fixed at their standard values. Errors on the structure constants are given as deviations from the central results. In the case of fits to N_f and $\alpha_s(M_{Z^0})$ with B_W the fits failed to converge and no results are quoted.

	$\mathcal{O}(\alpha_s^2)$+NLLA fits to C_A					$\mathcal{O}(\alpha_s^2)$+NLLA fits to C_F					$\mathcal{O}(\alpha_s^2)$+NLLA fits to N_f			
	$1-T$	M_H	B_T	B_W	all	$1-T$	M_H	B_T	B_W	all	$1-T$	M_H	B_T	all
central	**2.7**	**3.3**	**3.4**	**4.0**	**3.2**	**1.5**	**1.2**	**1.1**	**0.9**	**1.2**	**7.1**	**3.2**	**3.0**	**4.3**
$\alpha_s(M_{Z^0})$	0.128	0.110	0.110	0.090	0.112	0.115	0.127	0.129	0.134	0.122	0.132	0.109	0.109	0.113
$\Delta\alpha_s(M_{Z^0})$	±.019	±.016	±.019	±.014	±.012	±.033	±.032	±.038	±.028	±.019	±.016	±.018	±.020	±.012
χ^2/d.o.f.	2.9	3.3	2.6	0.4	11	3.0	3.1	2.9	0.4	10	2.7	3.4	2.5	11
stat.	±0.2	±0.1	±0.1	±0.2	±0.1	±0.2	±0.0	±0.0	±0.0	±0.0	±1.0	±0.5	±0.3	±0.3
expt.	±0.3	±0.2	±0.1	±0.0	±0.1	±0.2	±0.1	±0.1	±0.0	±0.0	±1.3	±1.3	±0.7	±0.4
Fit range	±0.5	±0.4	±0.3	±0.5	±0.3	±0.4	±0.2	±0.1	±0.1	±0.1	±1.3	±2.5	±1.6	±1.4
$a+1$ st.d.	-0.1	-0.2	-0.3	±0.0	-0.2	+0.1	+0.1	+0.1	+0.0	+0.1	+0.2	+1.4	+1.4	+1.2
$a-1$ st.d.	+0.1	+0.1	+0.1	+0.3	+0.1	-0.1	±0.0	±0.0	-0.1	-0.1	-0.7	-0.6	-0.6	-0.6
σ_q+1 st.d.	-0.1	-0.1	-0.1	+0.1	-0.1	+0.1	±0.0	±0.0	±0.0	±0.0	+0.1	+0.5	+0.3	+0.3
σ_q-1 st.d.	±0.0	+0.1	+0.2	+0.3	+0.1	±0.0	-0.1	-0.1	-0.1	-0.1	-0.3	-0.9	-0.8	-0.7
Peterson	-0.1	+0.1	-0.3	+0.1	±0.0	+0.1	-0.1	+0.1	±0.0	±0.0	+0.4	-0.7	+1.5	+0.2
udsc quarks	-0.1	+0.1	+0.6	+0.7	+0.2	+0.1	±0.0	+0.1	-0.2	-0.1	±0.0	-0.5	+1.4	-1.1
$Q_0=2$ GeV	-0.2	-0.2	-0.3	±0.0	-0.2	+0.2	+0.1	-0.2	±0.0	+0.1	+0.8	+0.9	–	+0.9
HERWIG 5.5	-0.1	+0.6	-0.5	+0.3	+0.2	+0.1	-0.2	+0.3	-0.1	-0.1	+0.3	–	+2.5	-0.9
ARIADNE 3.1	-0.2	-0.1	-0.5	-0.3	-0.2	+0.2	±0.0	+0.3	+0.1	+0.1	+0.6	+0.5	+2.6	+1.2
$x_\mu=0.5$	-0.1	-0.3	-0.2	-0.5	-0.2	+0.2	+0.1	+0.1	+0.1	+0.1	+0.1	+1.4	+0.9	+0.9
$x_\mu=2.0$	+0.1	+0.3	+0.2	+0.5	+0.2	-0.1	-0.1	-0.1	-0.1	-0.1	-0.2	-1.6	-0.9	-0.9
Total error	**±0.7**	**±0.9**	**±1.0**	**±1.1**	**±0.5**	**±0.6**	**±0.4**	**±0.5**	**±0.3**	**±0.3**	**±2.4**	**±3.9**	**±4.7**	**±3.0**

Table 7: Results of fits using the $\mathcal{O}(\alpha_s^2)$+NLLA calculations ($\ln(R)$-matching). One of the three structure constants and $\alpha_s(M_{Z^0})$ are allowed to vary in the fits while the other two structure constants are kept fixed at their standard values. Errors on the structure constants are given as deviations from the central results. In the case of fits to N_f and $\alpha_s(M_{Z^0})$ with B_W the fits failed to converge and therefore no results are quoted. In some cases fits from a particular systematic check did not converge and therefore no deviations due to these effects are quoted. Total errors are given for these cases but should be taken as lower limits (non-bold errors).
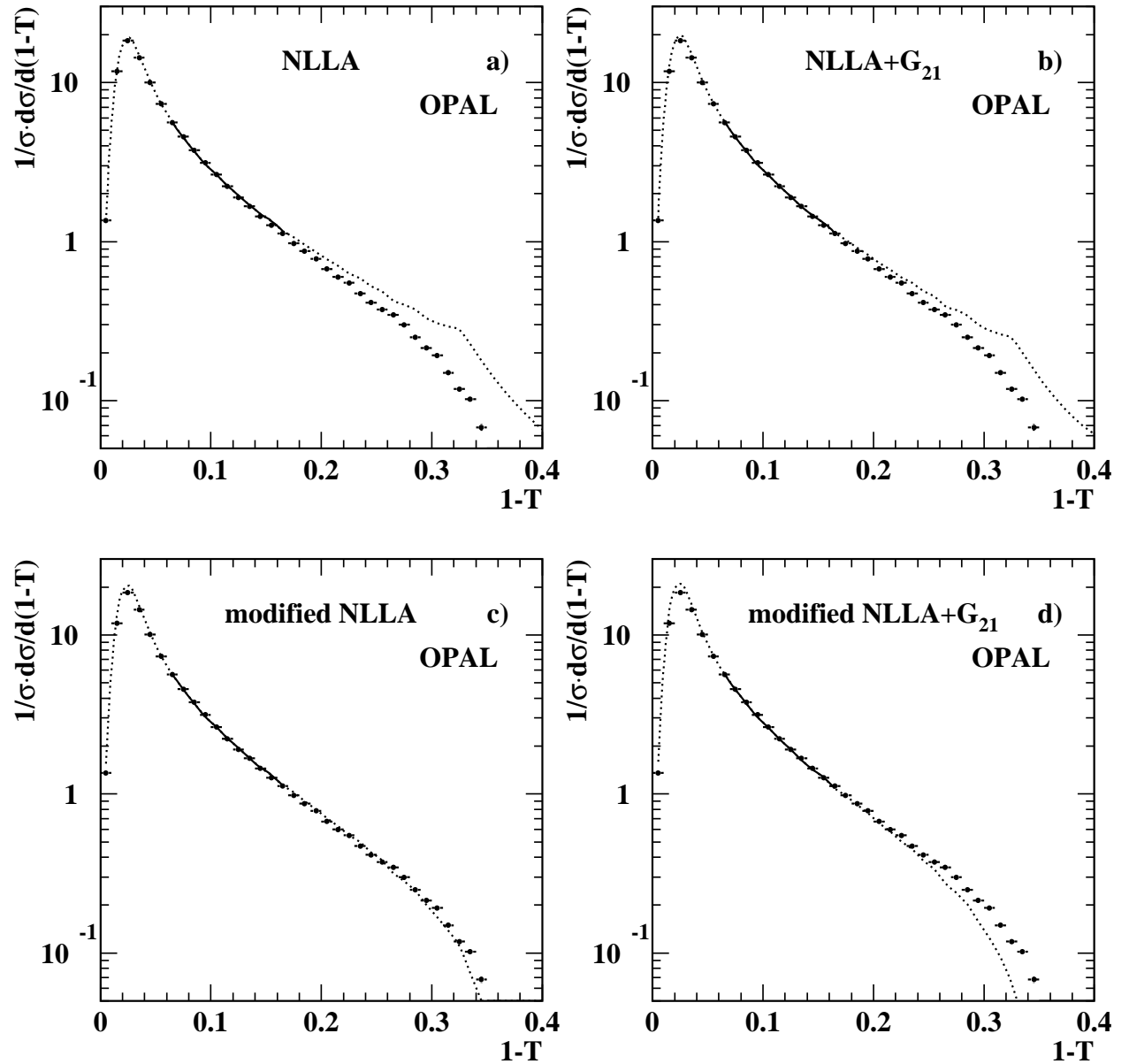
Figures

Figure 1: Fits based on NLLA QCD predictions with $x_\mu = 1$ compared with data for $1 - T$. The full lines indicate the fitted range and the dotted lines indicate an extrapolation using the fit results. The points are data corrected to the hadron-level. See text for an explanation of the different calculations used.
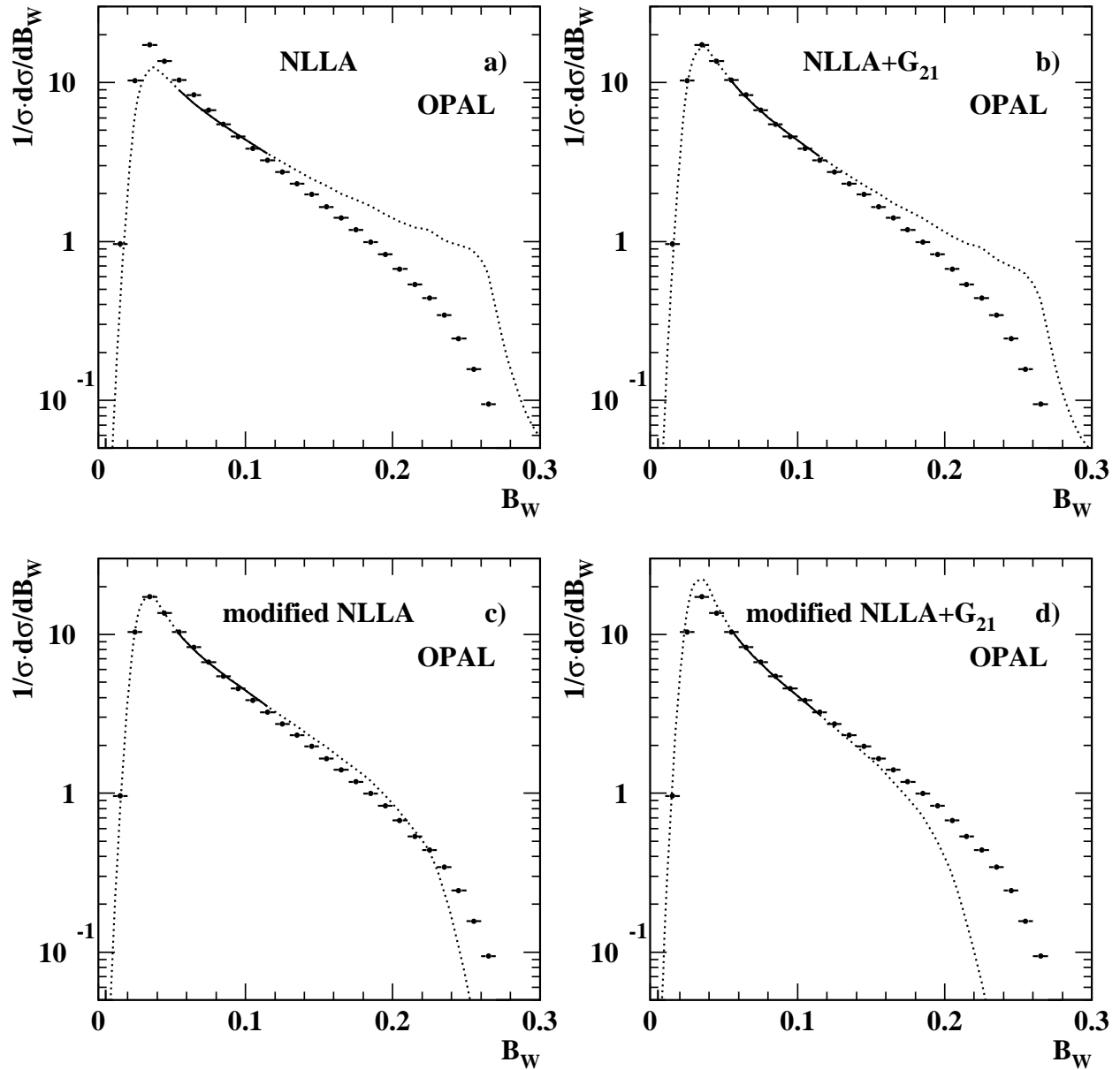
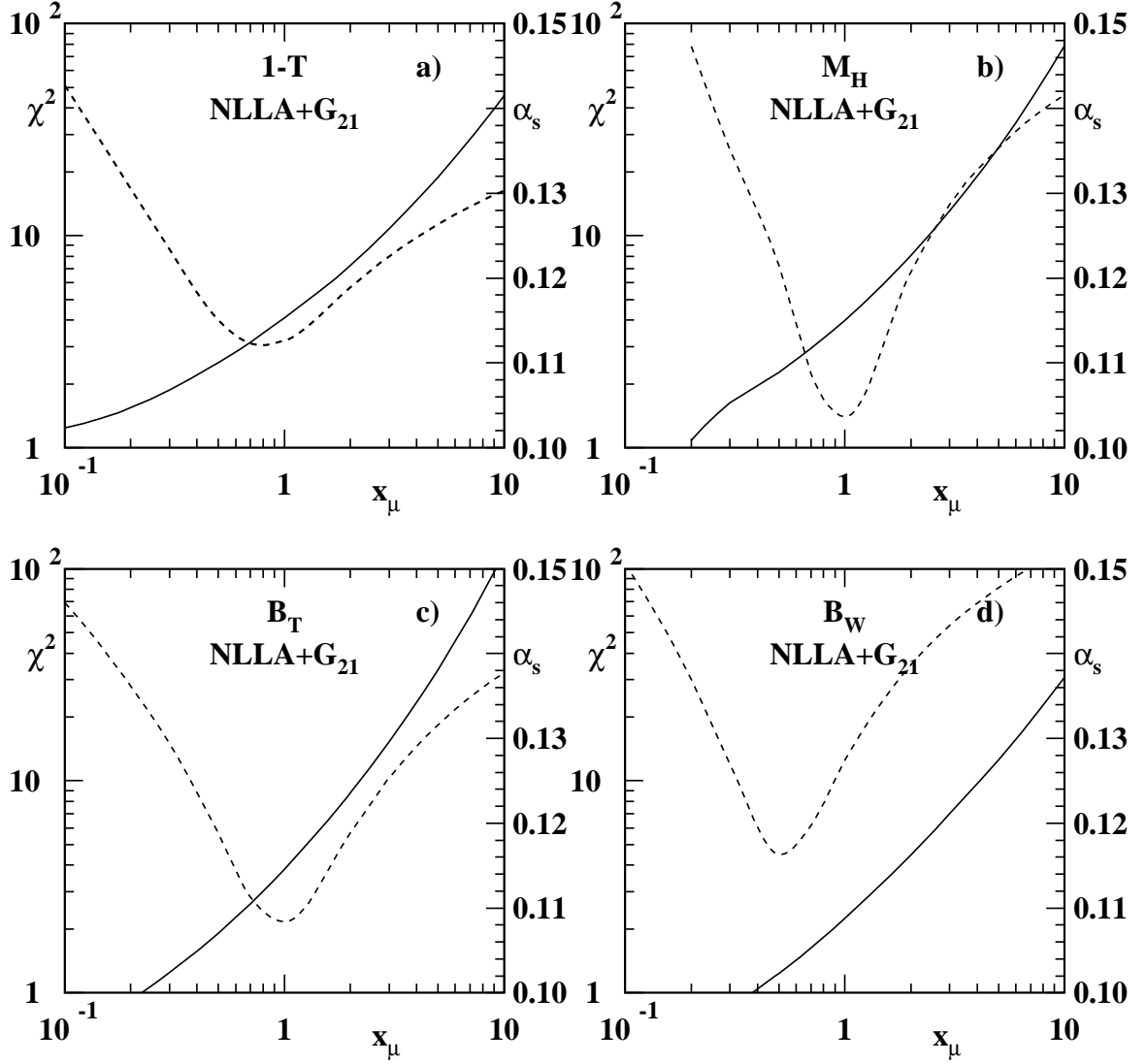Figure 2: Fits based on NLLA QCD predictions with $x_\mu = 1$ compared with data for B_W. The full lines indicate the fitted range and the dotted lines indicate an extrapolation using the fit results. The points are data corrected to the hadron-level. See text for an explanation of the different calculations used.

OPAL

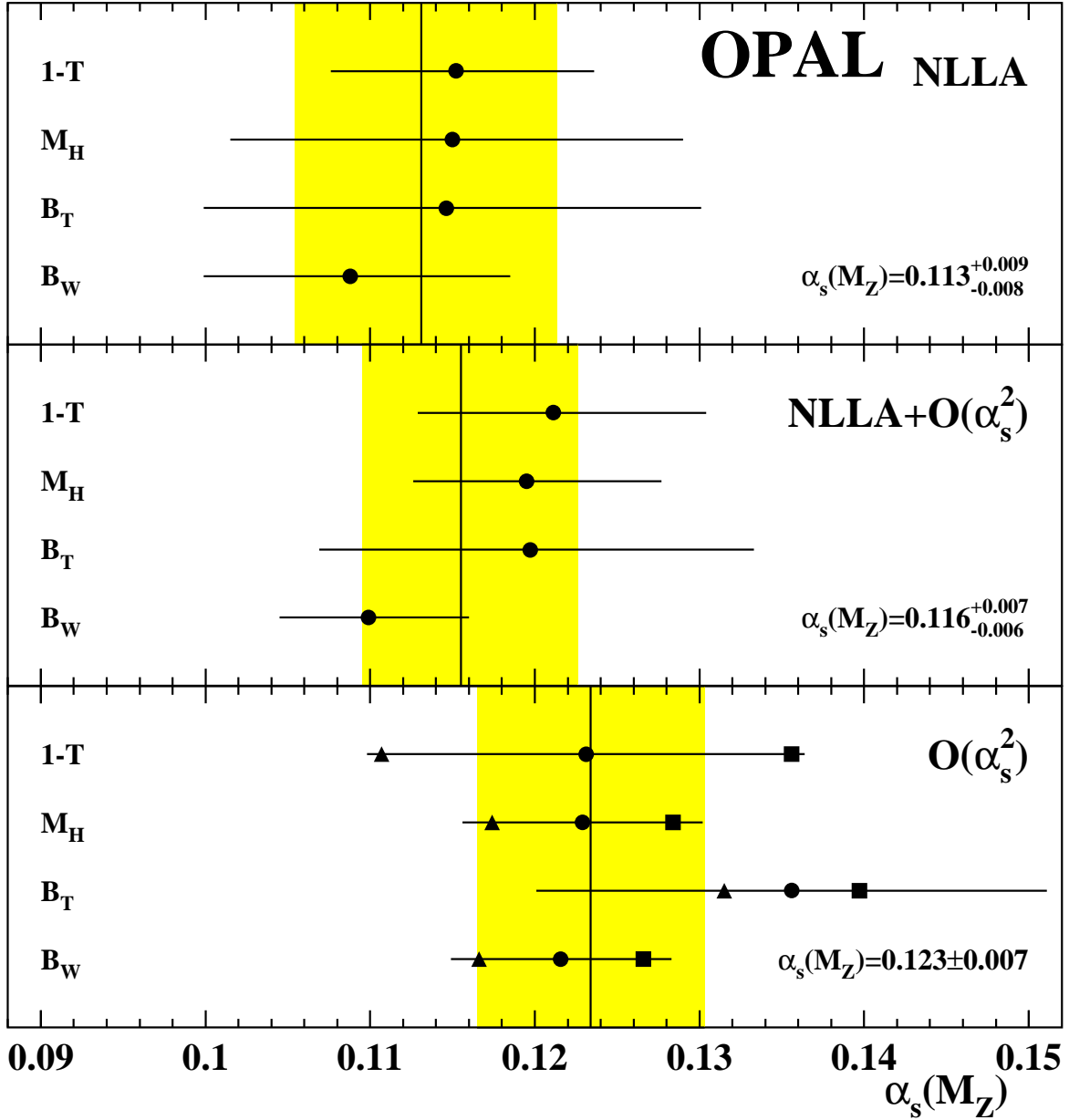Figure 3: Dependence of $\alpha_s(M_{Z^0})$ (solid curves) and χ^2/d.o.f. (dashed curves) on the renormalisation scale parameter x_μ for NLLA+G_{21} fits.

Figure 4: Comparison of measurements of $\alpha_s(M_{Z^0})$ using three different types of QCD calculation. The errors shown include all experimental and theoretical systematic contributions. The vertical lines and shaded bands indicate the combined results obtained by a simple weighted average and their errors. In the cases of fits including NLLA terms the results are based on $x_\mu = 1$ but in the case of $\mathcal{O}(\alpha_s^2)$ fits the central values (circles) represent an average of $\alpha_s(M_{Z^0})$ taking $x_\mu = 1$ (squares) and $\alpha_s(M_{Z^0})$ with x_μ free (triangles).
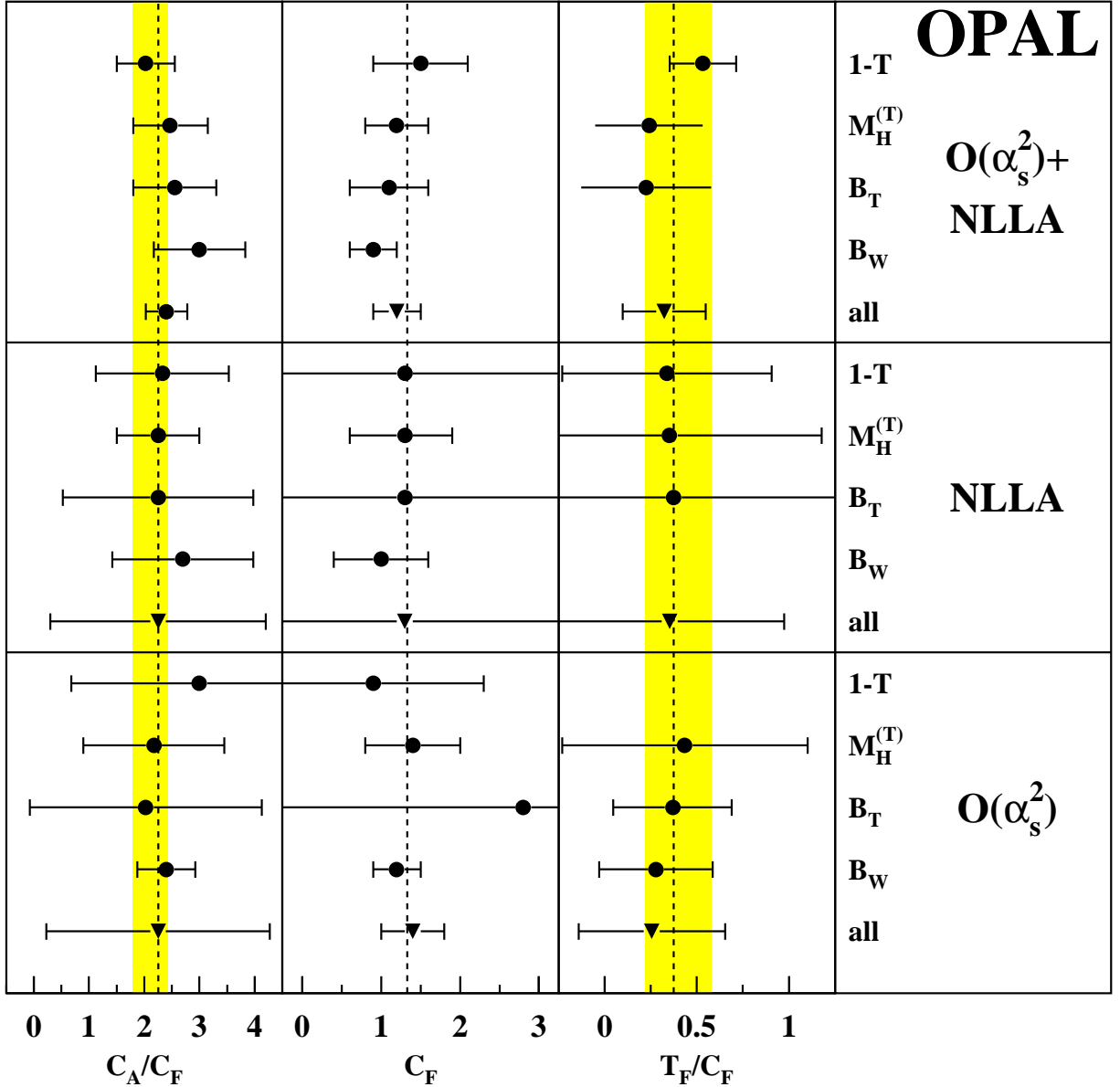
Figure 5: Results of fits to event shape observables varying $\alpha_s(M_{Z^0})$ and one of the three QCD structure constants C_A, C_F and T_F at a time with three different types of QCD calculations. The $\mathcal{O}(\alpha_s^2)$+NLLA calculation has been carried out using the $\ln(R)$-matching. For results from all observables the four distributions have been fitted simultaneously with a common $\alpha_s(M_{Z^0})$ and structure constant as free parameters. Fit results are shown by full points. In cases where error bars lack tick marks at the ends not all systematic checks are performed as explained in the text. Some of the large error bars are clipped. The dashed lines indicate the expectations from QCD, while the shaded boxes show the results from [7].
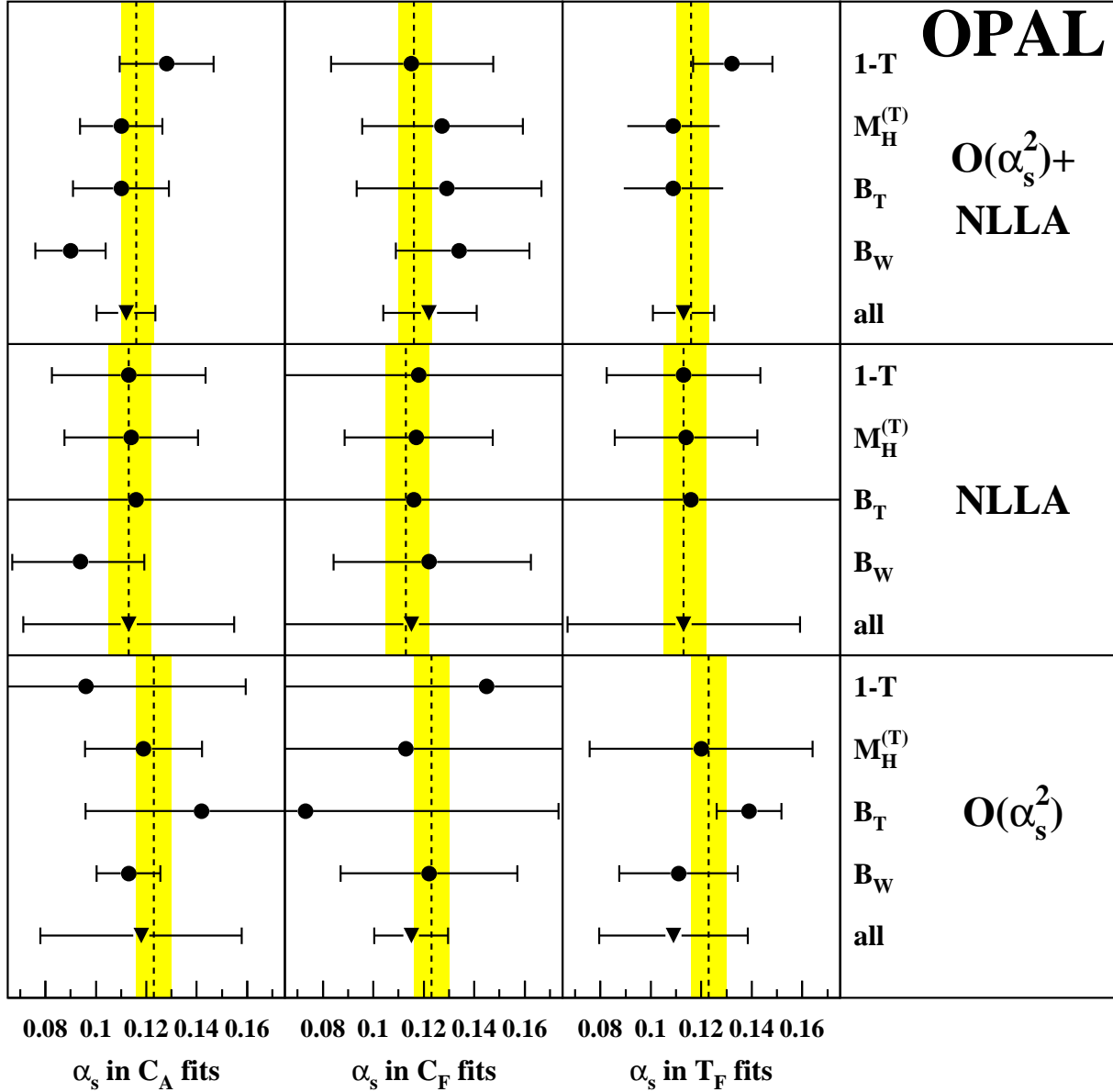
Figure 6: Results for $\alpha_s(M_{Z^0})$ from fits to event shape observables varying $\alpha_s(M_{Z^0})$ and one of the three QCD structure constants C_A, C_F and T_F at a time with three different types of QCD calculations. The $\mathcal{O}(\alpha_s^2)$+NLLA calculation has been carried out using the $\ln(R)$-matching. For results from all observables the four distributions have been fitted simultaneously with a common $\alpha_s(M_{Z^0})$ and structure constant as free parameters. Fit results are shown by full points. In cases where error bars lack tick marks at the ends not all systematic checks are performed as explained in the text. Some of the large error bars are clipped. The dashed lines and the shaded areas indicate values of $\alpha_s(M_{Z^0})$ as shown in figure 4 with the four observables and three types of QCD calculations considered here.
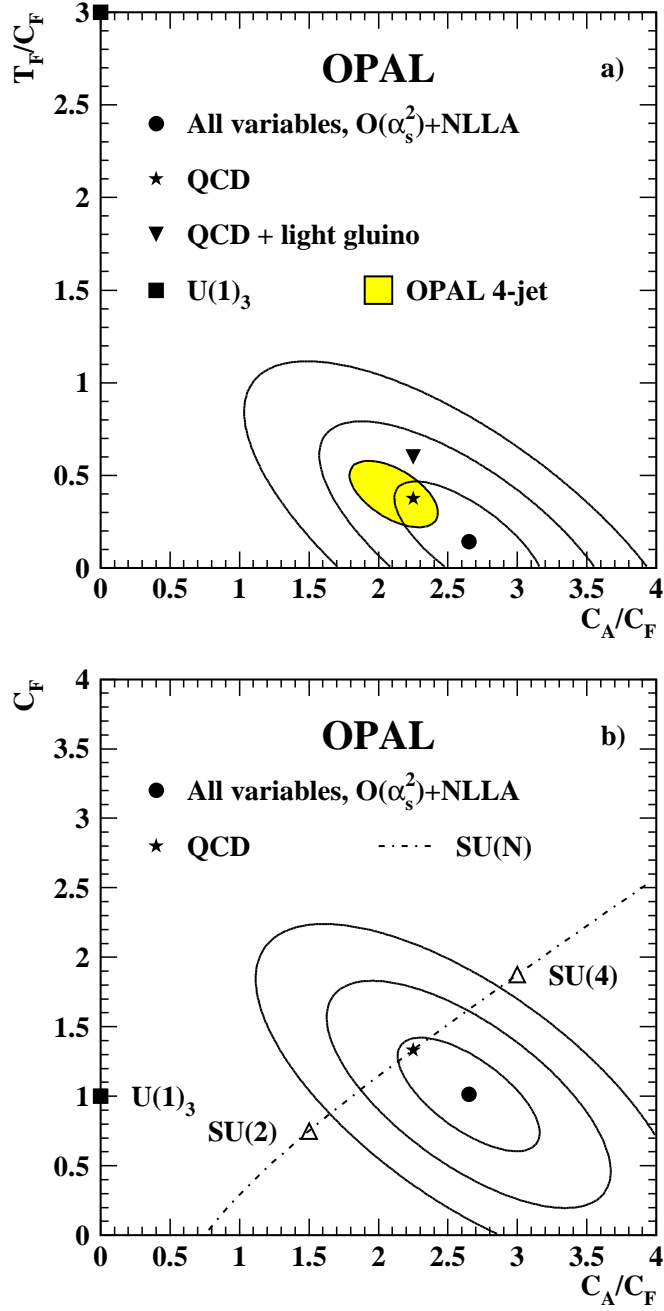
Figure 7: Error ellipses with T_F/C_F and C_A/C_F or C_F and C_A/C_F as fit parameters. The one, two and three standard deviation ellipses are drawn, corresponding to confidence levels of 39%, 86% and 99%, respectively. The shaded ellipse on figure a) shows the result from [7] as a one standard deviation contour. The dashed-dotted line on figure b) indicates the SU(N) constraint $C_F = (C_A{}^2 - 1)/(2C_A)$.